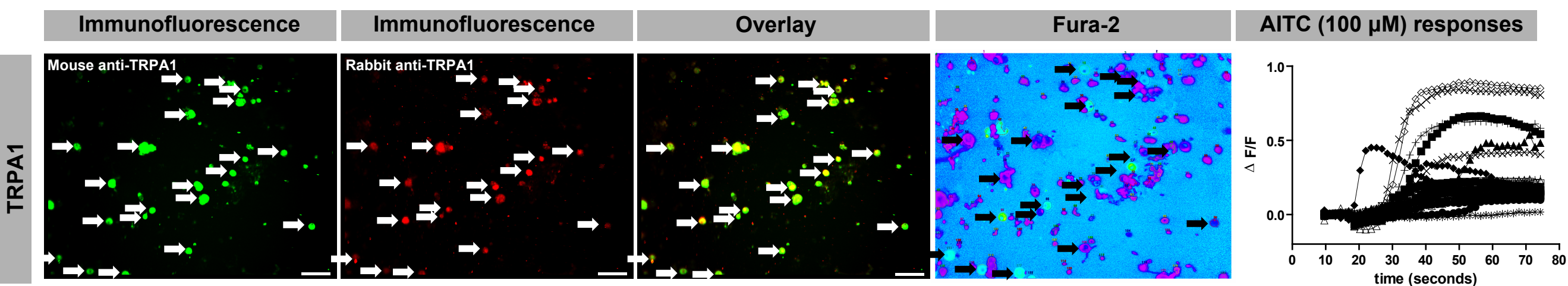
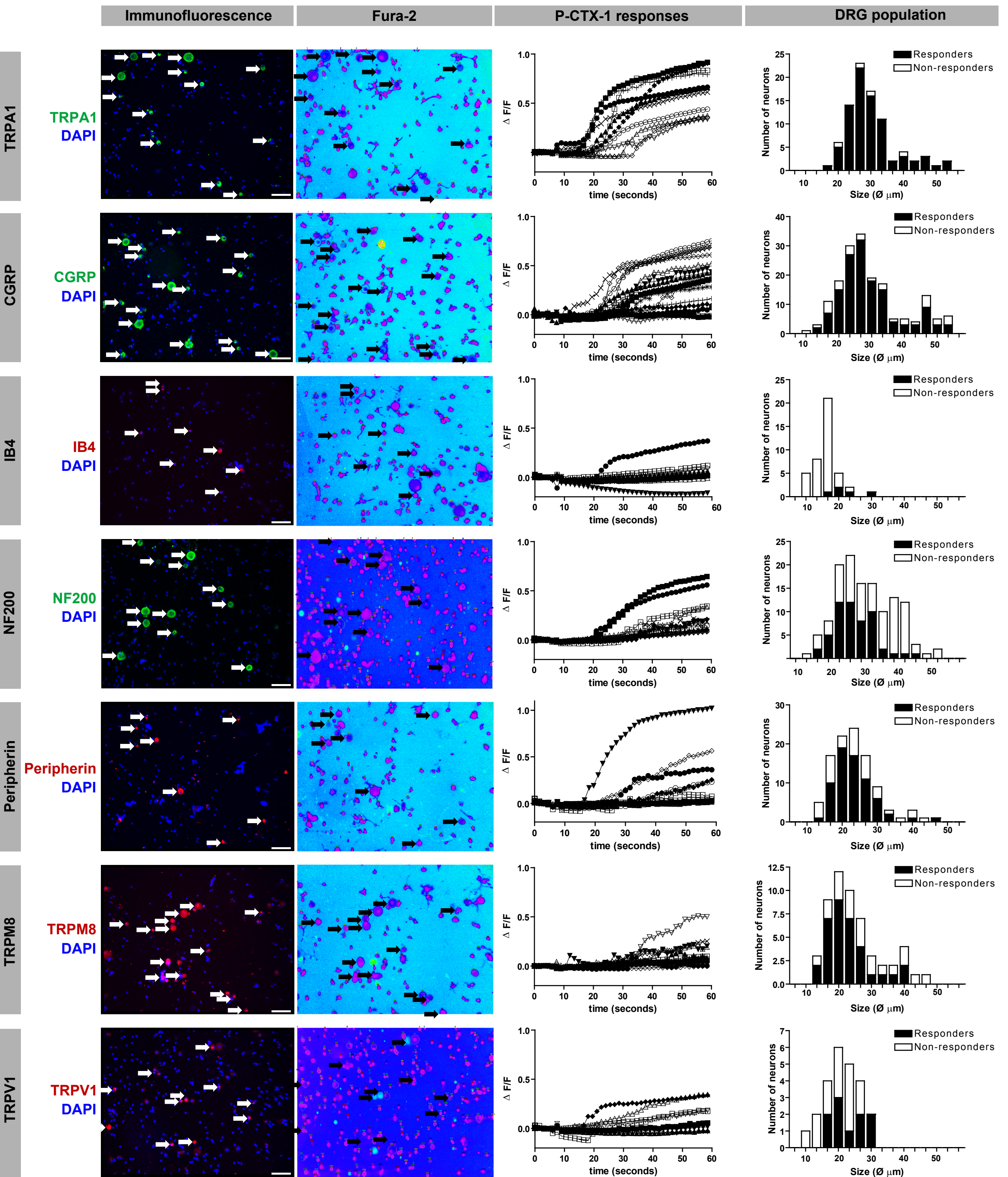
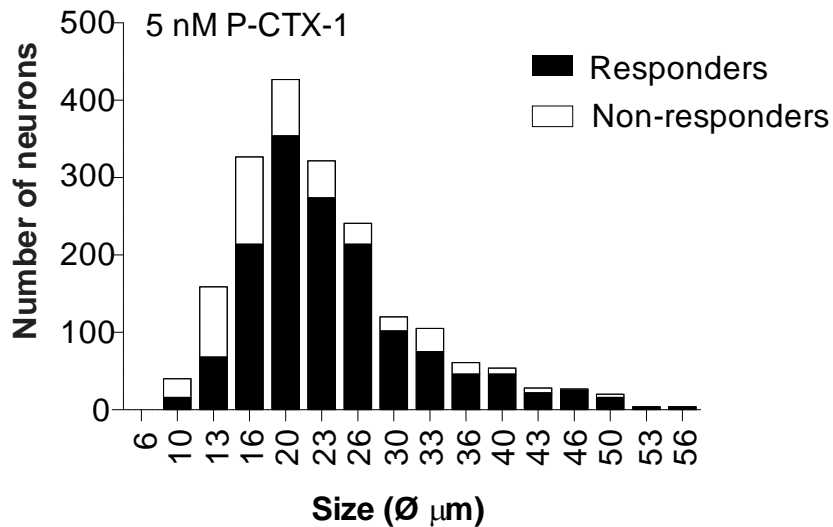


**Supplementary Fig. 1. Ciguatoxin does not affect mechanical thresholds.** (A) Paw withdrawal threshold to mechanical stimulation using von Frey hairs were determined 1 h after intraplantar administration of P-CTX-1 using an electronic von Frey apparatus (Bioseb, France). Treatment with P-CTX-1 did not affect mechanical thresholds compared to the buffer-injected contralateral paw. (B, C) Vector graph demonstrating the effect of P-CTX-1 on mechanical sensitivity assessed in the rat skin-nerve preparation using gravity-driven von Frey hairs. The mechanical threshold of C-fibers was not significantly affected by treatment with (A) 0.1 nM (n = 22) and (B) 1 nM (n = 16) P-CTX-1 (applied subsequently in the same units) although some of the fibers seemed to be sensitized (red arrows).



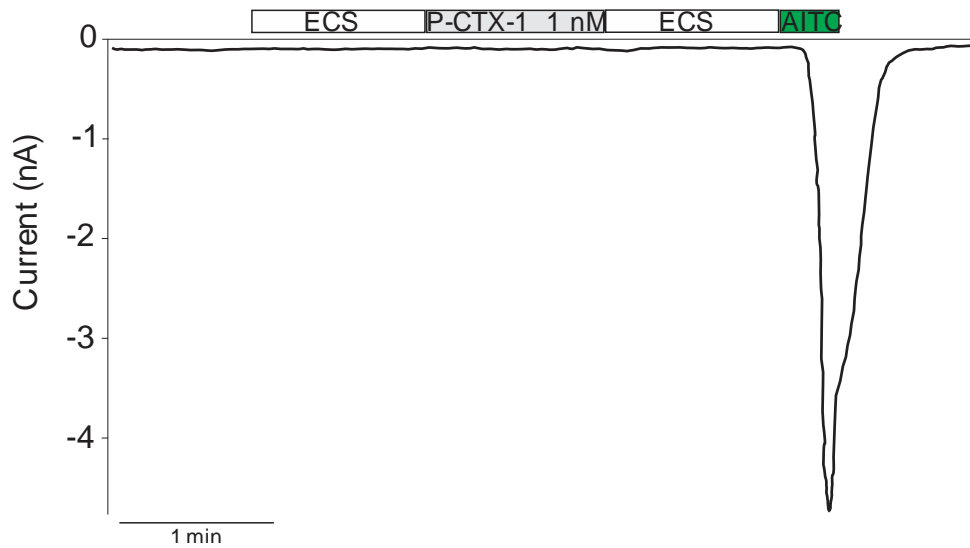
**Supplementary Fig 2. Immunochemical characterization of ciguatoxin-sensitive DRG populations.**  $\text{Ca}^{2+}$  responses to stimulation with 1 nM P-CTX-1 were measured using the BD Pathway 855 High Content Imaging Platform (BD) in Fura-2-loaded mouse DRG neurons, followed by immunochemical staining for TRPA1, CGRP, IB4, NF200, peripherin, TRPM8 and TRPV1. TRPA1- and CGRP-positive neurons were predominantly ciguatoxin-sensitive, with 159/166 (95 %) and 141/171 (82 %) of TRPA1- and CGRP-expressing cells, respectively, responding to P-CTX-1 (1 nM) with increases in intracellular  $\text{Ca}^{2+}$ . In contrast, the subpopulation of predominantly small, IB4-positive cells defined ciguatoxin-insensitive neurons, with only 13/106 (12 %) responding to P-CTX-1. NF200- and peripherin-positive neurons consisted of both ciguatoxin-sensitive and -insensitive neurons (54/129 (42 %) and 68/103 (66 %) P-CTX-1 responders, respectively). Similarly, TRPM8 and TRPV1 staining did not define ciguatoxin-sensitive neuronal populations, with only 34/54 (63 %) of TRPM8-positive neurons and 47/62 (76 %) of TRPV1-positive neurons responding to P-CTX-1.

Specificity of antibodies was confirmed through absence of staining in corresponding knockout animals (TRPM8, TRPV1, data not shown). In addition, specificity of the TRPA1 antibody was further confirmed by co-staining with an additional monoclonal mouse anti-TRPA1 antibody and positive association of staining with  $\text{Ca}^{2+}$  responses to AITC (100  $\mu\text{M}$ ). Overlay of rabbit and mouse anti-TRPA1 staining was excellent, and 17/25 TRPA1-positive cells responded with a  $\text{Ca}^{2+}$  increase of at least 15% to stimulation with AITC. Scale bar; 100  $\mu\text{m}$ .

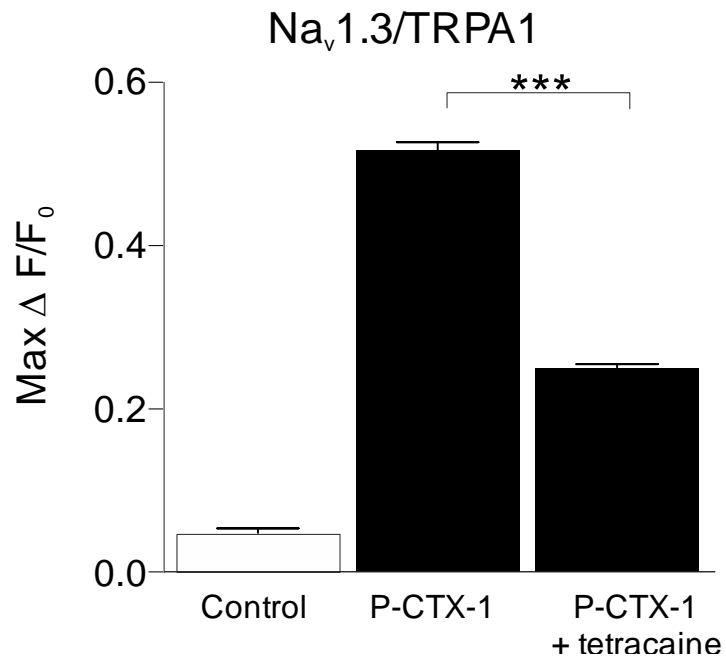


**Supplementary Fig 3. Quantification of ciguatoxin-sensitive DRG neurons.**

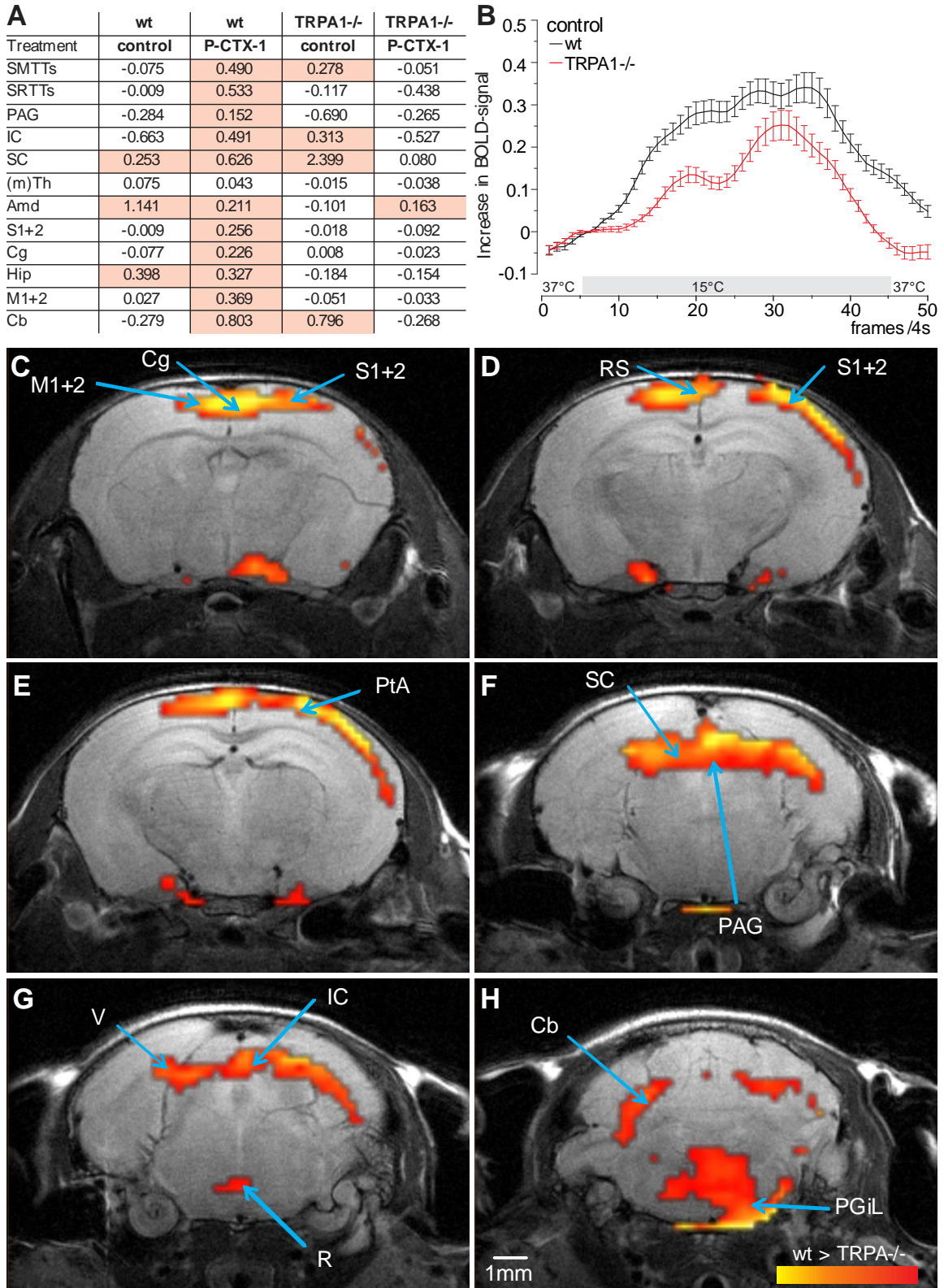
Ca<sup>2+</sup> responses to stimulation with 1 nM P-CTX-1 were measured using the BD Pathway 855 High Content Imaging Platform (BD) in Fura-2-loaded mouse DRG neurons (followed by immunochemical staining for TRPA1, CGRP, IB4, NF200, peripherin, TRPM8 and TRPV1). Black bars, P-CTX-1 responders; white bars, P-CTX-1 non-responders. Higher concentrations of P-CTX-1 were less discriminating and increasingly excited remaining neuronal populations, with 76% of DRG neurons excited by 5 nM P-CTX-1 in contrast to 51% at 1nM (compare main text and main Fig. 3).



**Supplementary Fig. 4. Effects of P-CTX-1 and allyl isothiocyanate (AITC) on currents of heterologously expressed hTRPA1.** Time course of inward TRPA1 currents recorded at a holding potential of -60 mV during application of P-CTX-1 and AITC. P-CTX-1 does not affect the TRPA1 current, while 200  $\mu$ M AITC induces a large inward current. Representative trace of  $n = 3$  individual recordings.



**Supplementary Fig 5. TRPA1-mediated calcium-responses in HEK cells expressing Na<sub>v</sub>1.3 and TRPA1 are blocked by tetracaine.** Treatment with the Na<sub>v</sub> antagonist tetracaine (100  $\mu$ M) inhibited Ca<sup>2+</sup> responses elicited by 10 nM P-CTX-1 in HEK293 cells co-expressing Na<sub>v</sub>1.3 and TRPA1 ( $p < 0.05$ ).



**Supplementary Fig 6. Functional MRI studies in *wt* and TRPA1<sup>-/-</sup> mice.** (A) Temporal change (slope) in the group average BOLD peak response per cold stimulus repetition. Based on the observation that repeated cold stimuli led to increasing amplitudes of BOLD signals after treatment with P-CTX-1, we analyzed the brain structures involved in these sensitized cold responses and found a strong positive correlation for mouse brain structures already described to be selectively involved in processing of heat and cold hypersensitivity in human functional imaging studies <sup>1, 2</sup>. Brain areas showing increased responses to consecutive cold stimuli are highlighted (green). Abbreviations: SMTTs, spino-mesencephalic tract; SRTTs, spino-reticular tract; PAG, periaqueductal gray; IC, inferior colliculus; SC, superior colliculus; (m)Th, medial thalamus; Amd, amygdala; S1+2, primary and secondary somatosensory cortex; Cg, cingulate cortex; Hip, hippocampus; M1+2, motor cortex; Cb, cerebellum. (B) Compared to *wt* animals (black timeline), TRPA1<sup>-/-</sup> mice (red timeline) showed an altered hemodynamic response function (HRF) in response to stimulation of the paw with 15°C. Changes in BOLD signal from n = 9-10 animals were averaged over 6 repetitive cold stimuli. Error bars represent S.E.M. (C-H) Second order statistical parameter maps showing differential brain activity (*wt* > TRPA1<sup>-/-</sup>) in response to cold stimulation in *wt* and TRPA1<sup>-/-</sup> animals, superimposed on the corresponding anatomical image. Activation was assessed by BOLD-fMRI. The yellow-red scale indicates increased activity in *wt* compared to TRPA1<sup>-/-</sup> animals. Arrows indicate regions with increased differential activity. For cold stimulation under control conditions, (C) the S1/S2 somatosensory cortex, the cingulate (Cg) cortex and the motor (M1/2) cortex, (D) the retrosplenial cortex (RS), (E) pretectal area (PtA), (F) superior colliculus (SC), periaqueductal gray (PAG), (G) visual cortex (V), inferior colliculus (IC), raphe nucleus (R) (H) cerebellum (Cb) and lateral paragigantocellular nucleus (PGiL) show significantly higher activity in *wt* than TRPA1<sup>-/-</sup> mice. Data are presented as mean ± SEM.



**Supplementary Table 1. Primary antibodies used to characterize ciguatoxin-sensitive neurons**

Name	Host	Antigen Characteristics	Catalog no.; Source	Dilution	Reference
Neurofilament Heavy Chain (NF200)	Rb; p	Full length native protein	Ab8135; Abcam, Cambridge, MA	1:1000	(53, 54)
Peripherin	Ck; p	Recombinant protein expressed in bacteria	Ab39374; Abcam, Cambridge, MA	1:500	(55)
Calcitonin gene-related peptide (CGRP)	sheep; p	Synthetic rat $\alpha$ -CGRP	BML-CA1137-0025; Biomol; Hamburg, Germany	1:1000	(56)
TRPV1	Gp; p	C-terminus of rat TRPV1 (YTGSLKPEDAIEVFKDS MVPGEK)	GP14100; Neuromics, Edina, MN	1:1000	(57, 58)
TRPM8	Rb; p	short peptide of N-terminus of TRPM8	KAL-KM060; CosmoBio, Carlsbad, CA	1:500	(12, 59)
TRPA1	Rb; p	TRPA1 partial recombinant protein	Ab58844; Abcam, Cambridge, MA	1:1000	(60, 61)
TRPA1	Ms; m	clone 6G8; partial recomb. protein with GST tag (IPNADKSLEMEILKQK YRLKDLTFLLEKQHELI KLIQKMEIIESETEDDDS HCSFQDRFKKEQMEQR NSRWNTVLRAVKAKT HHL)	WH0008989M3 Sigma Aldrich, Castlehill, NSW, Australia	1:1000	
Isolectin B4 (IB4)	N/A	Lectin; Griffonia simplicifolia B4 subunit binding to $\alpha$ -D-galactosyl residues	I21412; Invitrogen, Carlsbad, CA, USA	1:500	(62)
Neuron-specific $\beta$ 3-tubulin	Ms; m	Biotin, Clone TuJ-1, Mouse IgG2A	BAM1195 R&D Systems, Minneapolis, MN, USA	1:1000	(63)

**Abbreviations:** aa, amino acids; Rb, rabbit; Ck, chicken; Gp, guinea pig; Ms, mouse; p, polyclonal; m, monoclonal

**Supplementary Table 2: Characteristics of C- and A-fibers recorded from *wt*, *TRPA1*<sup>-/-</sup> and *Nav1.8*<sup>-/-</sup> mice.**

genotype	subtype	conduction velocity (average, range)	von Frey threshold (median, range)	n
<i>wt</i>	C-fibers	0.42 m/s (0.21- 0.55 m/s)	5.7 mN (4-45mN)	10
<i>wt</i>	A-fibers	10.59 m/s (3.40-16.56 m/s)	1 mN (1-5.4 mN).	15
<i>TRPA1</i> <sup>-/-</sup>	C-fibers	0.48 m/s (0.29-1.26 m/s)	5.7 mN (4-32mN).	12
<i>TRPA1</i> <sup>-/-</sup>	A-fibers	10.69 m/s (4.11-18.66m/s)	1.4 mN (1-8 mN)	15
<i>Nav1.8</i> <sup>-/-</sup>	C-fibers	0,49 m/s (0.37-0.59 m/s)	11.4 mN (5.7-11.4mN)	6